The Effects of Ore Properties on the Characterization of Suspension in Settling and Compression

Majid Unesi [1*], Mohammad Noaparast [2], Sied Ziaedin Shafaei [2], Esmaeil Jorjani [1]

1. Department of mining Engineering, Science and Research branch, Islamic Azad University, Tehran, Iran

2. School of Mining Engineering, University of Tehran, Tehran, Iran

Abstract

Many studies have considered the effects of suspension properties on the dewatering process but few have focused on ore properties. Thus, the present work studied the effects of ore properties (density, particle size, mineralogy) on the dewatering process based on lab and pilot experiments. A hydrocyclone was used to prepare the required samples for the experiments. To study the effects of mineralogical properties, the sedimentation behaviour of hydrocyclone feed and underflow samples were compared. It was observed that the free-settling velocity of feed (2 to 6mm/sec) was less than in the underflow sample (2 to 7mm/sec) and the final concentration of underflow sample (0.45 to $0.48t/m^3$) was more than the feed sample (0.44 to $0.47t/m^3$). Additionally, to study the effects of particle size and density, the sedimentation behaviour of hydrocyclone overflow and feed samples were compared. The settling velocity and final concentration of overflow sample were obtained at 0.15 to 0.4mm/sec and $0.32t/m^3$, respectively, which was significantly less than the feed sample. This was due to the amount of clay reduction in the underflow sample and particle size and density reduction in the overflow sample. Following on, the pilot experiments were carried out. It was observed that the bed formation of the feed sample tended to overflow in the sample at low flux ($10t/m^2/day$) and tended to underflow in the sample at high flux ($28.5t/m^2/day$). This meant that the long time at lower flux created an opportunity for fine particles to settle easily, similar to coarser particles and as such, ore properties did not play a decisive role in bed formation, but their effects appeared instead at higher flux. Furthermore, it was observed that the underflow concentration increased by decreasing the flux from 28.5 to $10t/m^2/day$. These increasing amounts were $0.05t/m^3$ and $0.12t/m^3$ in hydrocyclone overflow and underflow samples, respectively, at a height of 2.5 metres. This meant that the compressibility and permeability of the hydrocyclone underflow sample was much better than in the hydrocyclone overflow sample, which was clearly a result of the ore properties (density, particle size, mineralogy).

Keywords: *compression, ore properties, settling, thickener.*

1. Introduction

Mineral processing techniques are performed in environments that contain a significant amount of water and the majority of this water is removed with tailings. Thus, it is necessary to use dewatering equipment such as thickeners in order to avoid environmental contamination. Paste thickeners can minimize the volume of water ultimately consumed and reduce the volume of solid waste requiring disposal. Schemes such as thickened tailings disposal and paste fill all involve the deposition of dewatered tailings to improve water recovery and decrease tailings volumes and costs [1-9]. 'Paste' is a term for a suspension of solids that are relatively non-settling and non-segregating. Furthermore, paste has a self-supporting structure and when deposited on the ground will form a slope of varying inclinations, depending on the solids concentration. Paste properties are produced by the relatively high suspended solids concentrations [10-14]. Several models and experiments have been presented by researchers to understand the thickening process and for predicting the relationship among the process parameters [15]. Different thickening theories have been proposed by Coe and Clevenger (1916), Kynch (1952), Talmage-Fitch (1955), Yoshioka-Hotta (1957), Adorjan (1976), Oltmann-Osborne (1977), Wilhelm-Naide (1981), Dahlstrom-Fitch (1985), Yalcin (1988), Kelly-Spottiswood (1989) and others [15-18]. Furthermore, chemical engineers have developed several models to simulate dewatering behaviour by [19-21]. A 1-D model of dewatering was developed by Buscall and White (BW, 1987), which quantifies the solids volume fraction, the compressive yield stress and the hindered settling function [15]. Furthermore, Landman and White (1988, 1994) used the phenomenon model to describe the solid flux function and effective solid stress. They determined the subjected forces on particles in the sedimentation and consolidation process [22-23]. The BW theory developed by Green (1997), properly modelled the comprehensive yield stress and hindered settling function in the suspension bed, but not sedimentation above the bed [24]. The Kynch theory was developed by Garrido (2003) who modelled the sedimentation-consolidation process [25]. The Green (1997) theory was developed by

De Krester (2003) and presented a relationship between the bed-depth and concentration [26]. Garrido and Burger (2003) also developed software for the design and simulation of batch- and continuous-thickening [27]. Furthermore, an algorithm was developed by Usher et al. (2005) to account for the underflow concentration and sediment bed of fundamental suspension properties [28]. This algorithm could not predict suspension properties in the shear process; Gladman (2005) improved this model by shearing the suspension, but did not consider aggregate densification [29]. Following on, Slotee (2005) presented the relationship between paste yield stress and particle size [30-32]; Nasser (2007) developed the Landman theory (1994) and investigated the effect of pH and electrolyte on thickener performance [33]. The suspension dewatering equations were developed by Usher and Scales (2009), based on the aggregate densification, whereby aggregate compacted and became smaller when subjected to forces in thickening process. They were modelled the liquid flow velocity around and through aggregates [34]. The validation of the Usher algorithm was studied by Gladman et al. (2010), who found that this model was most accurate at the shortest residence times and lowest bed heights, but less accurate for longer residence times and higher beds. This was due to changes in the dewatering properties of flocculated aggregates over time, which had not been adequately considered in the Usher algorithm [35]. Doucet (2010) understood that rise rate, resident time and bed depth were important parameters on paste thickener design [36]. Lester (2010) developed the 2-dimensional model of BW, using continuity, separation and transport equations in its modelling. Since it was difficult to solve this model computationally, a CFD method was used for modelling [37]. Van Deventer (2011) developed the Kynch theory, which was based on aggregate densification behaviour. Therefore, aggregate densification theory was used to predict the final equilibrium bed height by densification rate and bed compression. Moreover, the relationship between aggregate size and thickening time was obtained [38].

Most of the studies above focused on the effects of suspension properties in the dewatering process; however, few studies

have considered the effects of ore properties on the dewatering process. Thus, the aim of the current research was to study the effects of ore properties such as solid density, particle size and mineralogy on the thickening process in order to better understand dewatering behaviour and to present the nature of suspension in settling and compression.

2. Materials and Methods

Tailings samples from the Sarcheshmeh copper flotation plant in Iran were used in all experiments. As the hydrocyclone could separate particles based on their density and size, the tailings samples were initially and continuously introduced to a hydrocyclone via a centrally located pipe, thereby separating the tailings into two products as overflow and underflow samples. The particle size analysis and XRD test was carried out using these samples. The laboratory screens and a cyclosizer were used for particle size analysis, and the results are presented in Table 1. Solid density was determined using a pycnometer ($100cm^3$) and the results are presented in Table 2, along with XRD analysis.

Table 1. Particle size analysis.

	Feed	Overflow	Underflow
d_{80} (micron)	120	22	130
d_{75} (micron)	105	20	110
d_{50} (micron)	40	8	47
d_{25} (micron)	8	2	11

Table 2. XRD analysis and solid density of samples.

Minerals	Hydrocyclone Feed	Hydrocyclone Overflow	Hydrocyclone Underflow
Aluminum Silicate (ClinoChlore, Illite, Chamosite, Anorthite) (%)	75.6	80.5	70.4
Quartz: SiO2 (%)	22	17	26.5
Pyrite: FeS2 (%)	2.5	2.3	3.1
Solid Density (g/cm3)	2.8	2.7	2.8

To study the effect of ore properties on the thickening process, various experiments on the plant conditions for all samples were conducted. The samples were taken as a suspension from the hydrocyclone and were treated by waste water tailings, so that the thickening behaviour could only be attributed to ore properties. The samples were prepared to the required concentration, based on experimental conditions. In addition, the sample pH was 11, equal to industrial pH. A high molecular weight anionic polyacrylamide (NF43U from SNF) was then used to flocculate the suspension and prepare it at $0.25g/dm^3$, which is the industrial dosage. A $500cm^3$ cylinder was employed to study thickening behaviour and a chronometer was used to record the mud lines at different times in laboratory scale.

The Plexiglass pilot column was 4m in height and 0.2m in internal diameter. The feed and flocculent were introduced at a column height of approximately 3m via a feed-well by peristaltic pump. Additionally, the dilution water was introduced at the same column height. Overflow was collected by a peripheral launder. The interface between the feed and clarified water could be observed. Suspensions were transferred to a hydrocyclone equipped with overflow and underflow boxes. Based on each experiment's conditions, the hydrocyclone overflow, underflow or feed were transferred to the pilot column.

Shortly after filling the column, three zones became distinguishable. The top of the column was characterized by a clarified zone. In the middle zone, individual aggregates could be observed to settle and the lower zone was an opaque region in which solids settled at a slower rate. There was a marked interface between the middle and lower zones, termed here as the ''bed height'' or "bed depth". It should be noted that this was not necessarily the point at which solids became networked. Several column experiments were undertaken and for each run, the column was allowed to operate for a sufficient time to reach the steady state, before sampling commenced. On this basis, steady state conditions took anywhere between 2 to 5 hours, depending on the bed height. After this time had elapsed, underflow samples were collected at 15 minute intervals.

No solids were recorded in the overflow for any conditions used in the experiments and the supernatant was always observed to be clear.

3. Result and Discussion

Since the amount of flocculent consumption in the paste thickeners was usually between 20 and 40gpt, the laboratory tests were carried out with a wider range of rate, between 15 and 60gpt; however, the pilot tests were performed on 25gpt. To study the sedimentation behaviour of the samples, a series of experiments were conducted in laboratory and pilot scales and the results are presented below.

3.1. Laboratory scale

A series of experiments were performed and the sedimentation curves are accordingly presented in Figures 1 to 3. As shown in Table 2, the highest amount of feed was composed of clay minerals and quartz, and the highest amount of the hydrocyclone overflow sample was composed of clay minerals; the highest amount of quartz and metallic minerals was transferred to the hydrocyclone underflow sample. To study the mineralogical behaviour of the samples, the sedimentation experiments of hydrocyclone feed and underflow samples were compared. As can be seen in Figures 1 and 3, the free-settling velocity of the feed sample was less than in the hydrocyclone underflow sample at different flocculent dosages and in the compaction zone, the final concentration of hydrocyclone underflow sample (0.45 to $0.48t/m^3$) was higher than in the feed sample (0.44 to $0.47t/m^3$). This stemmed from the reduction of clay content in the hydrocyclone underflow sample.

According to the measurements and calculations, the solid mass fraction of hydrocyclone overflow and underflow were 10% and 90% of feed, respectively. Moreover, as per Figure 1, it was observed that a good concentration was obtained in the compaction zone by increasing the flocculent dosage to 30gpt. However, excessive flocculent dosage caused a reduction in bed concentration for the feed sample and accordingly, the final height values in the settling curve were increased to 64mm (for 20gpt) and 68mm (for 60gpt). The cotton-mode formed in this zone was the result of an increase in flock's

sizes, because the networked water remained inside the flocks. This case was also observed in the underflow sample (Fig. 3). A good concentration was obtained in the compaction zone by increasing the flocculent dosage to 25gpt in the hydrocyclone underflow sample and decreasing the height value to 62.5mm.

By increasing the flocculent dosage more than 25gpt, the cotton mode was observed in the compaction region. This may have been due to interactions between particles in the feed and hydrocyclone underflow samples. Since there was a significant difference between feed and hydrocyclone overflow samples in terms of ore properties, a large difference was also found between their settling velocities (Fig. 4). A settling velocity between 0.15 and 0.4mm/sec was obtained for the overflow sample; this was between 2 and 6mm/sec for the feed sample (Fig. 4). As per Figures 1 and 2, the final height for the feed and overflow samples were about 64mm and 92mm, respectively. In other words, the final concentration for the feed sample was higher than for the hydrocyclone overflow sample, which was dependant on ore properties. The cotton accumulation of flocks (Fig. 1) was also observed in the overflow sample.

In order to compare the settling flux, the Wilhelm-Naide theory was applied and the results are given in Figure 5. The maximum settling flux for hydrocyclone underflow, overflow and feed samples were obtained at 9, 0.23 and $12.5t/m^2/hr$, respectively. Additionally, the maximum concentrations in the underflow were obtained at 0.46, 0.32 and $0.48t/m^3$, respectively. In other words, the maximum settling flux and final concentration of hydrocyclone underflow and overflow samples were more and less than the feed sample, respectively. The initial flux values of the hydrocyclone overflow sample had been severely changed. This meant that the flocculent could not prevail in the initial turbulence that had been created, due to the low settling velocity of the hydrocyclone overflow sample. This behaviour was observed for a low dosage of flocculent in the feed sample (15gpt). Thus, the minimum amount of required flocculent will be obtained by studying the resistance between initial turbulence and settling velocity, which can be achieved in the settling flux curve.
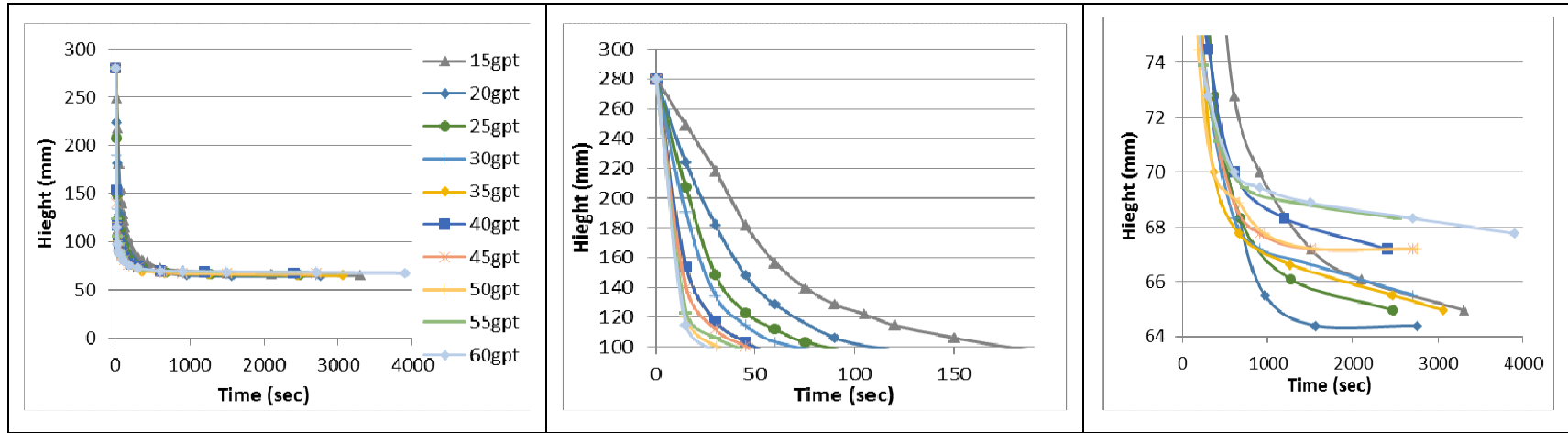
Fig. 1. Feed sedimentation curves, left: overall view, centre: the linear part, right: the end part.
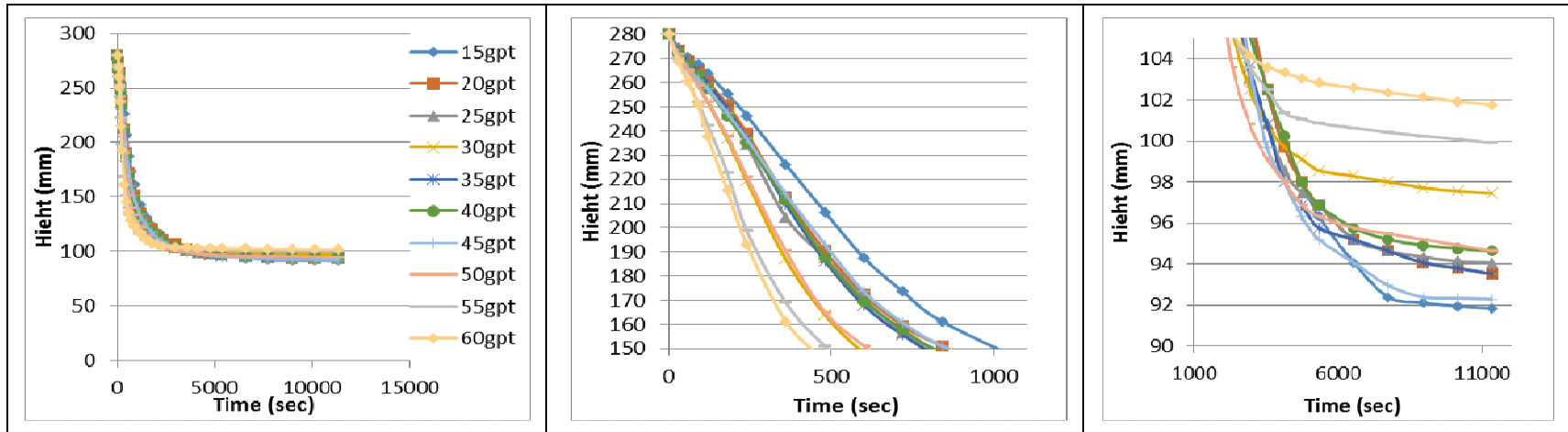

Fig. 2. Hydrocyclone overflow sedimentation curves, left: overall view, centre: the linear part, right: the end part.
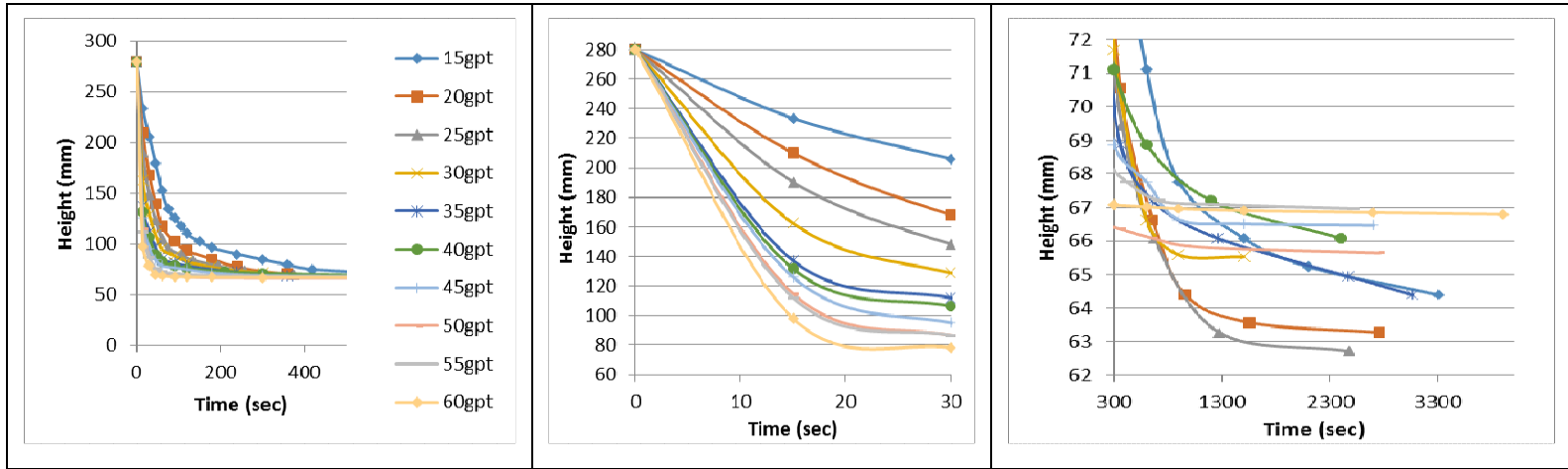
Fig. 3. Hydrocyclone underflow sedimentation curves, left: overall view, centre: the linear part, right: the end part.
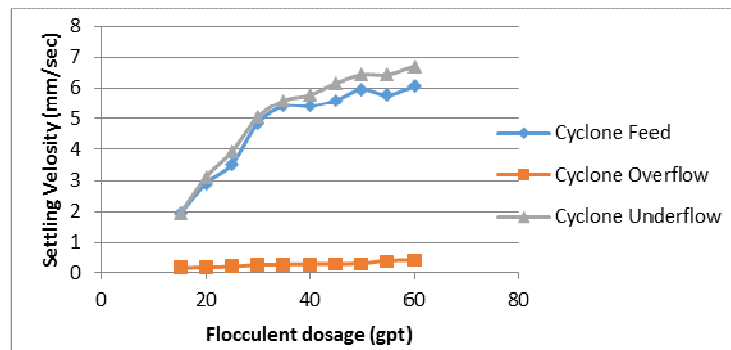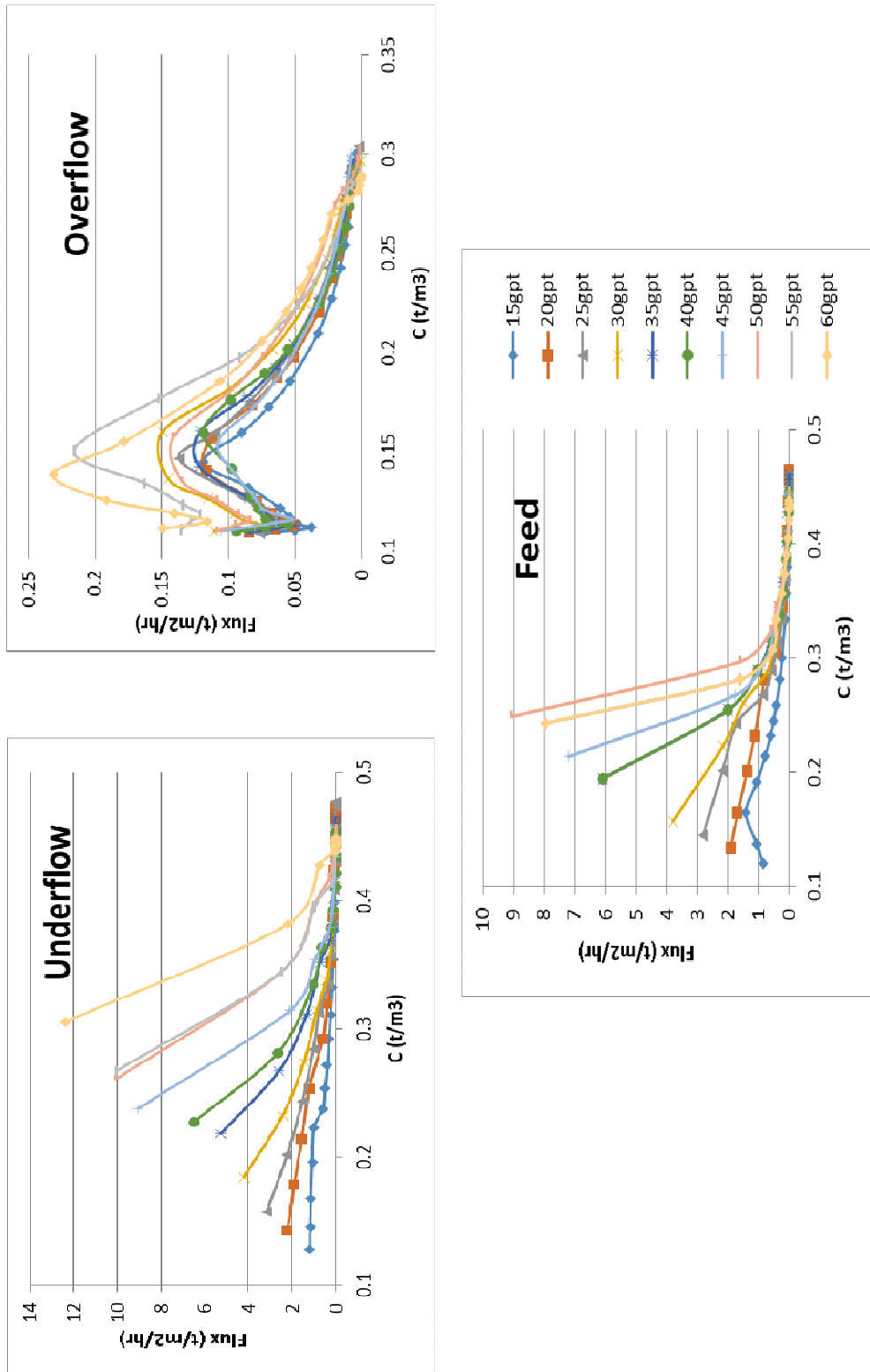

Fig. 4. Free-settling curves of samples.

Fig. 5. The settling flux in different underflow concentrations.

3.2. Pilot scale

3.2.1. The batch tests

The batch tests were conducted in the start-up phase. After column start-up was completed, the bed of solids began to form and the relevant interface could be readily detected (by eye). The bed height gradually increased as solids accumulated and when the solid bed reached the desired height (0.5 to 2.5m), the time was recorded using a chronometer. Figure 6 presents the bed formation curves, where the column was discontinuously operated at different fluxes. The bed formation for the feed sample tended towards the overflow curve at low flux (10t/m^2/day) and to the underflow curve at high flux (28.5t/m^2/day). In other words, the longer time at lower flux created an opportunity for fine particles to settle easily. Therefore, the high solid density and particle size did not play a decisive role in bed formation, their effects instead appearing at higher flux. In addition to flux, the bed formation depended on the compressibility caused by smooth slope changes in some parts of the curves. The bed compression usually occurred at a 2 to 2.5 m height. This was not observed in the hydrocyclone overflow and underflow samples, except in the hydrocyclone overflow sample with a higher flux (28.5t/m^2/day). This was repeated in the feed sample, which may have been due to the coarser and finer particle interactions or the interaction of clay, quartz and metallic minerals. Therefore, it was postulated that the particle size distribution and the dominant minerals in the samples would cause this effect. Furthermore, it was observed that the bed formation rate of fine particles was faster than for coarse particles, while the free-settling velocity of fine particles was slower. This was due to the packing of particles on top of each other during settling. Clays and finer particles typically stacked into a honeycomb structure. Honeycomb-packing retained large amounts of water, as water filled the voids formed by the honeycomb structure and it was therefore not sufficiently compacted.
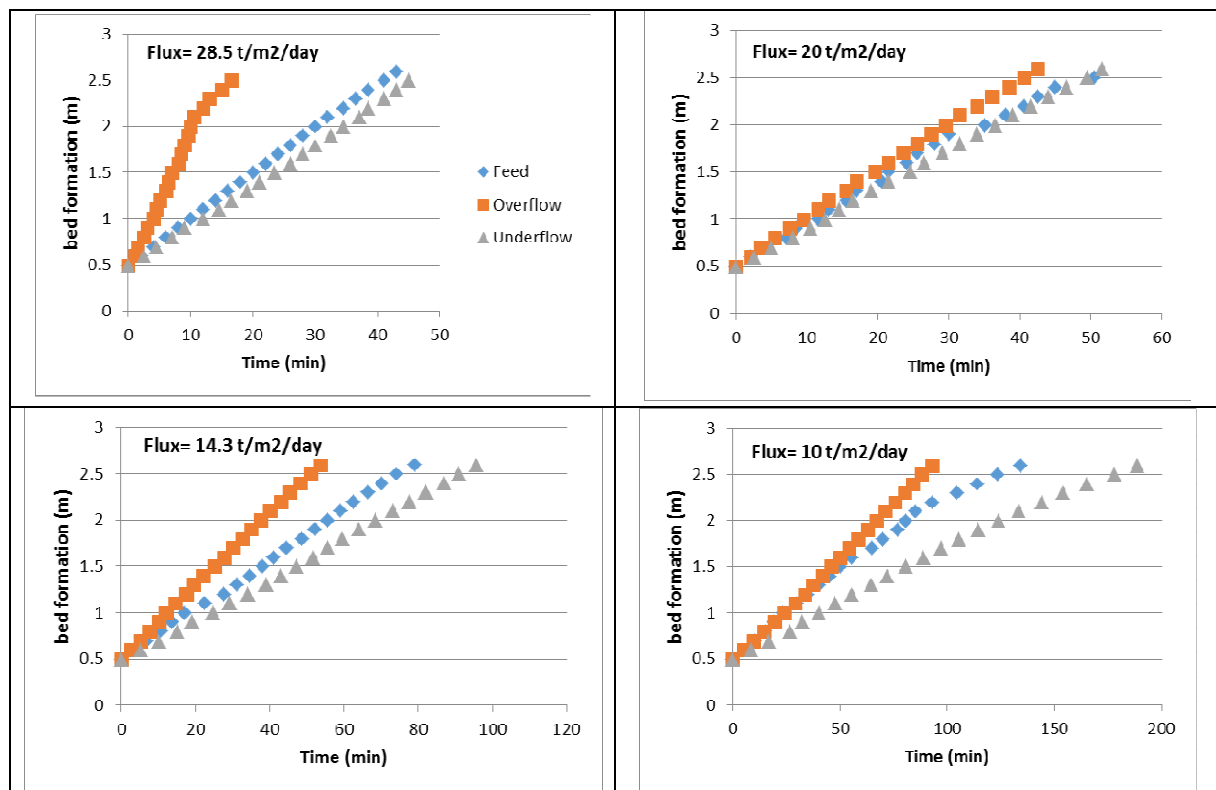

Fig. 6. The bed formation curves for different fluxes.

3.2.2. The continuous tests

For the continuous tests, several column experiments were performed. The results of solids flux, bed height and ore properties for each run are presented in Figure 7 and Table 3. The bed height was allowed to increase to approximately 80% of the target height, at which point the underflow pump was turned on. This was done to compensate for the slow dynamic response in the column. In practice, the underflow pump speed needed to be periodically adjusted to keep the bed height constant, due to variations in underflow solid content. Therefore, the underflow rate varied with the variation of the underflow pump speed for controlling the bed height. Over the course of a run, the bed height was maintained within 10% of the nominal height. In the first period of time for each run, the average underflow rate increased, which corresponded to a decrease in underflow solid concentration as the system moved to the steady state. Furthermore, the underflow solid content was initially unsteady. After some time, this fluctuation faded away and the underflow solid content remained fairly constant. For each run, the column was allowed to operate for a sufficient time in order to achieve the steady state prior to sampling commencing. On this basis, the steady state conditions took anywhere from two to five hours, depending on the bed height. Once this period of time had elapsed, column underflow samples were collected at 15 minute intervals. No solids were recorded in the overflow for each condition used in the experiments and the supernatant was always observed to be clear. Results for the experiments are presented below.
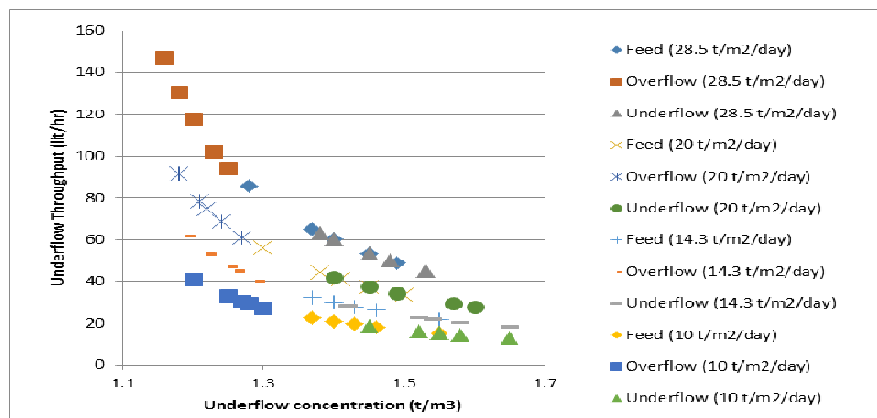

Fig. 7. Underflow throughput as a function of underflow concentration at different fluxes and bed depths.

Table 3. The underflow concentration at different bed heights and fluxes.

Flux (t/m2/day)	height (m)	Feed	Overflow	Underflow	Flux (t/m2/day)	Feed	Overflow	Underflow
	0.5	1.28	1.16	1.38		1.37	1.19	1.42
	1	1.37	1.18	1.4		1.4	1.22	1.52
28.5	1.5	1.4	1.2	1.45	14.3	1.43	1.25	1.54
	2	1.45	1.23	1.48		1.46	1.26	1.58
	2.5	1.49	1.25	1.53		1.55	1.29	1.65
	0.5	1.3	1.18	1.4		1.37	1.2	1.45
	1	1.38	1.21	1.45		1.4	1.25	1.52
20	1.5	1.41	1.22	1.49	10	1.44	1.27	1.55
	2	1.45	1.24	1.57		1.46	1.28	1.58
	2.5	1.5	1.27	1.6		1.56	1.3	1.65

3.2.2.1. Settling flux and underflow concentration

The variation of thickener underflow throughput versus underflow concentration at different fluxes and bed height are shown in Figure 7. The underflow throughput of the hydrocyclone overflow sample was higher than in the hydrocyclone underflow and feed samples at different fluxes. This was due to the rapid bed formation in the hydrocyclone overflow sample. Additionally, the difference between underflow throughputs for the hydrocyclone overflow sample at different flux was higher than for the other two samples. For instance, the underflow throughput at a settling flux of 28.5 and $10t/m^2/day$ was 94 and 27lit/hr, respectively, at a height of 2.5 m, the difference for which was 67lit/hr. On the other hand, the underflow throughput for the hydrocyclone underflow sample was 45 and 13lit/hr, respectively, the difference for which was 32lit/hr; the reason for this was because the compressibility of the hydrocyclone underflow sample was higher than for the hydrocyclone overflow sample.

In addition to compressibility, permeability was the other effective parameter on the paste thickener's performance. This parameter was much more evident in at higher flux. The bed height had little effect on the underflow concentration at high flux; this was because there had not been enough time for compression in the thickener and underflow concentration was dependent on permeability. In this case, the thickener worked based on underflow throughput and settling rate. Thus, thickener performance decreased and the changes in ore properties were able to severely affect thickener performance. The packing of particles on top of one another during settling influenced rheology and the solid content of the thickened underflow. The most familiar packing type is referred to as "edge-face," also known as the "house of cards," "face-face," and "band structure" packing relationship [39]. Clays and finer particles, of which there were more in the HO sample, typically stacked into a honeycomb structure. Honeycomb-packing retains large amounts of water, as water fills the voids formed by the honeycomb structure. Great effort and highly effective dewatering systems are required to remove this interstitial water, and thickener performance is decreased when this type of packing occurs.

Since the permeability of clay was very low, the thickener performance was expected to decrease when increasing the clay content in the ore. In this case, the lower flux was preferred, because by doing so the retention time increased and caused the thickener performance to increase. The bed depth had a significant effect on increasing the underflow concentration at lower flux. In the hydrocyclone overflow sample, decreasing the flux from 28.5 to $10t/m^2/day$ caused an increase in the underflow concentration from 1.25 to $1.3t/m^2/day$ at a height of 2.5 m. Furthermore, this phenomenon was observed in the hydrocyclone underflow sample, which had a lower amount of clay content. In this sample, decreasing the flux from 28.5 to $10t/m^2/day$ caused an increase in the underflow concentration from 1.53 to $1.65t/m^2/day$ at a height of 2.5 m. The increase in the thickener underflow concentration in the hydrocyclone overflow sample was $0.05t/m^3$ and $0.12t/m^3$ in hydrocyclone underflow sample. This meant that the compressibility and permeability of the hydrocyclone underflow sample was much better than in the overflow sample.

As stated above, the solid mass fraction of hydrocyclone overflow and underflow were 10% and 90% of feed, respectively. The underflow concentration of hydrocyclone feed and underflow samples at a settling flux of $14.3t/m^2/day$ was 1.55 and $1.65t/m^3$, respectively, at a height of in 2.5 m. This significantly increased the underflow concentration; additionally, this effect was observed at other fluxes. Therefore, ore properties can be seen to play a decisive role in paste thickener performance. It was observed on batch tests that the thickening behaviour of the feed sample tended toward the overflow curve at low flux ($10t/m^2/day$) and toward the underflow curve at high flux ($28.5t/m^2/day$). However, in continuous tests, the behaviour of the feed sample on underflow concentration tended toward the behaviour of the hydrocyclone underflow sample at high flux ($28.5t/m^2/day$), and tended toward both the hydrocyclone overflow and underflow samples' behaviour at

low fluxes. The impact of aluminosilicates on underflow concentration increased by decreasing the flux to 14.3t/m^2/day; further flux decreasing did not have a significant effect on underflow concentration.

3.2.2.2. Bed depth

As noted above, decreasing flux impacted underflow concentration and bed depth; however, this impact was limited and further flux reduction removed this effect. This issue was considered in the feed sample at 10 and 14.3t/m^2/day. As shown in Table 3, the underflow concentration for both fluxes at a 2.5 m height was 1.55t/m^3 and at other heights (0.5, 1, 1.5 and 2 m) were 1.37, 1.4, 1.43 and 1.46t/m^3, respectively. This behaviour was observed in all bed depths for the feed sample and in over one metre bed depth for the hydrocyclone underflow sample; it was not observed in the hydrocyclone overflow sample. It can be assumed that this behaviour will be observed at a height of more than 2.5 m or less than 10t/m^2/day fluxes for the hydrocyclone overflow sample. This sample needs further time to be compressed, which can be obtained at a higher depth or lower flux. Additionally, further pressure will apply at higher depths.

It is therefore understood that there was a difference in the flocks' network formation, which occurred due to particles' interaction. This interaction provided a link between bed depth and underflow concentration, which had not been observed in previous studies. This phenomenon therefore depends on ore properties such as particle size, solid density and mineralogy (clay content, quartz and metallic minerals). Based on the above, optimum flux and bed depth can be obtained for the desired underflow concentration in thickener design.

3.2.2.3. Fractional water recovery

The fractional water recovery was defined as the water overflow flow rate divided by the total flow rate of water fed to the column, assuming that all solids left via the underflow. Table 4 shows that a higher bed depth and lower flux increased water recovery, and that the fractional water recovery of the hydrocyclone underflow sample was higher than in the overflow sample. For example, the water recovery for the hydrocyclone feed, overflow and underflow samples at 20t/m2/day flux and a height of 2.5m were 63.80%, 63.36% and 69.23%, respectively. Therefore, the fractional water recovery would be an alternative method for determining thickener performance.

Table 4. The fractional water recovery in different bed heights and fluxes.

Flux (t/m2/day)	Height (m)	Feed	Overflow	Underflow	Flux (t/m^2/day)	Feed	Overflow	Underflow
	0.5	24.41	33.41	42.51		46.19	45.02	49.45
	1	46.19	41.58	46.15		51.27	53.46	62.13
28.5	1.5	51.27	48.11	53.85	14.3	55.64	59.87	64.10
	2	58.23	55.78	57.69		59.44	61.68	67.64
	2.5	62.77	59.87	63.13		68.35	66.36	72.78
	0.5	30.38	41.58	46.15		46.19	48.11	53.85
	1	47.97	50.91	53.85		51.27	59.87	62.13
20	1.5	52.79	53.46	58.87	10	55.64	63.36	65.03
	2	58.23	57.91	66.80		59.44	64.91	67.64
	2.5	63.80	63.36	69.23		69.16	67.71	72.78

4. Conclusion

- It was concluded that ore properties can significantly affect thickener performance (free-settling velocity and final concentration).

It was observed that the free-settling velocity of feed (2 to 6mm/sec) was less than in the hydrocyclone underflow sample (2 to 7mm/sec) and the final concentration of the

hydrocyclone underflow sample (0.45 to 0.48t/m^3) was higher than in the feed sample (0.44 to 0.47t/m^3). Additionally, the settling velocity and final concentration of the overflow sample were obtained as 0.15 to 0.4mm/sec and 0.32t/m^3, respectively, which was significantly less than for the feed sample. This was due to the amount of clay reduction in the underflow sample and particle size and density reduction in the overflow sample.

- The bed formation behaviour of the feed sample tended toward the overflow sample at low flux (10t/m^2/day) and toward the underflow sample at high flux (28.5t/m^2/day) in intermittent pilot tests. In other words, the longer time at lower flux caused an opportunity for fine particles to settle easily. Therefore, high solid density and particle size did not play a decisive role in bed formation at lower flux, but their effects were noted at higher flux.

- The underflow throughput of the hydrocyclone overflow sample was higher than for the hydrocyclone underflow and feed samples at different flux, which was due to the rapid bed formation and lower compressibility in this sample.

- Permeability was another effective parameter and was more evident at higher flux, because there was not enough time for compression to occur in the thickener. In this case, the thickener functioned based on underflow throughput and settling rate. Thus, thickener performance will be decreased and changes in ore properties can severely affect the thickener's performance.

- The underflow concentration increased by decreasing the flux from 28.5 to 10t/m^2/day. The amounts to which the concentration was increased in the hydrocyclone overflow and underflow samples at a height of 2.5m were 0.05t/m^3 and 0.12t/m^3, respectively. Additionally, the underflow concentration for the hydrocyclone feed and underflow sample at 14.3t/m^2/day was 1.55 and 1.65t/m^3, respectively, at a height of 2.5m. This meant that the compressibility and permeability of the hydrocyclone underflow sample was much better than for the overflow sample.

References

[1] Maurice C., Fuerstenau and Kenneth N.H. (2003). Principles of Mineral Processing Handbook, SME, pp. 340-343.

[2] Jewell, M.J., Fourie, A.B. and Lord, E.R. (2002). Paste and Thickened Tailings: A Guide, Australian Centre for Geomechanics, Perth.

[3] Slottee, J.S. and Johnson, J. (2009). Paste Thickener Design and Operation Selected to Achieve Downstream Requirements, 12th International Seminar on Paste and Thickened Tailings.

[4] September, N. and Kirkwood, R. (2010). Clermont Coal Mine Project Selection of Tailings Paste Thickener AusIMM – Technical Meeting, SKM.

[5] Mular, A., Halbe, D.N. and Barratt, D.J. (2002). Mineral Processing Plant Design, Practice and Control Proceedings, SME, Littelton Colorado USA, pp. 1295-1331.

[6] www.metsominerals.com, brochure (2011).

[7] Perry, H.R. (1999). Chemical Engineering Handbook, McGraw-Hill Companies, part 18 (gravity sedimentation operations).

[8] www.outotec.com, paste brochure, February (2011).

[9] Sofra, F. and Boger, D.V. (2001). Slope Prediction for Thickened Tailings and Paste, Tailings and Mine Waste, Proceedings of the 8th International Conference on Tailings and Mine Waste, Fort Collins. Balkema, Rotterdam, pp.75– 83.

[10] Newman, P. and Landriault, D. (1997). The Use of Paste Technology in the Surface Disposal of Mineral Waste, Waste Minimisation and Recycle, Birmingham.

[11] Meggyes, T. and Debreczeni, A. (2006). Paste Technology for Tailing Management, Land Contamination & Reclamation, 4, pp.815-827.

[12] www.dorrolivereimco.com, brochure, (2004).

[13] Arbuthnot, I., Garraway, B., Triglavcanin, R., Edwards, T., Colwell, D. and Roberts, K. (2005). Designing for paste thickening, Proceedings of the Canadian Mineral Processors, pp. 597-628.

[14] Cincilla, W.A., Landriault, D.A. and Verburg, R. (1997). Application of Paste Technology to Surface Disposal of Mineral Wastes, Tailings and Mine Waste, Proceedings of the Fourth

International Conference on Tailings and Mine Waste, Fort Collins, Colorado. Balkema, Rotterdam, pp. 343– 356.

[15] Buscall, R., McGowan, I.J., Mills, P.D.A., Stewart, R.F., Sutton, D., White, L.R. and Yates, G.E. (1987). The Rheology of strongly flocculated suspensions, Non-Newtonian Fluid Mechanics, 24, pp. 183–202.

[16] Svarovsky, L. (2000). Solid-Liquid Separation Handbook, Oxford, Boston, Butterworth-Heinemann, pp. 166-190.

[17] Rushton, A., Ward, A.S. and Holdich, R.G. (1996). Solid-Liquid Separation Technology Handbook, VCH, pp. 221-256.

[18] Gupta, A. and Yan, D.S. (2006). Mineral Processing Design and Operation, Perth, Australia, pp. 401- 437.

[19] Bürger, R., Bustos, M.C. and Concha, F. (1999). Settling velocities of particulate systems: 9. Phenomenological theory of sedimentation processes: numerical simulation of the transient behavior of flocculated suspensions in an ideal batch or continuous thickener. International Journal of Mineral Processing, 55, pp. 267–282.

[20] Concha, F., Bustos, M.C. and Barrientos, A. (1996). Phenomenological Theory of Sedimentation, Chapter 3 in Sedimentation of small particles in a viscous Fluid, Computational Mechanics Publications, Southampton, UK, pp. 51-96.

[21] Bustos, M.C., Concha, F., Burger, R. and Tory, E.M. (1999). Sedimentation and Thickening, Kluwer Academic Publishers, Dordrecht, Netherlands, p. 285.

[22] Landman, K.A., White, L.R. and Buscall, R. (1988). The Continuous-Flow Gravity Thickener: Steady State Behavior, AIChE Journal, 34, pp. 239-252.

[23] Landman, K.A. and White, L.R. (1994). Solid/liquid separation of flocculated suspensions, Advanced Colloid Interface, 51, pp. 175–246.

[24] Green, M.D. (1997). Characterization of Suspensions in Settling and Compression, PhD thesis, Department of Chemical Engineering, University of Melbourne Parkville Victoria 3052, Australia.

[25] Garrido, P., Concha, F. and Burger, R. (2003). Settling Velocities of Particulate Systems: 14

Unified model of sedimentation, centrifugation and filtration of flocculated suspensions, International Journal of Mineral Processing, 72, pp. 57– 74.

[26] De Kretser, R.G., Boger, D.V. and Scales, P.J. (2003). Compressive Rheology: an overview. Rheology Reviews, British Society of Rheology, pp. 125–165.

[27] Garrido, P., Burgos, R., Concha, F. and Bürger, R. (2003). Software for the design and simulation of gravity thickeners, Minerals Engineering, 16, pp. 85–92.

[28] Usher, S.P. and Scales, P.J. (2005). Steady State Thickener Modeling from the Compressive Yield Stress and Hindered Settling Function, Chemical Engineering Journal, 111, pp. 253–261.

[29] Gladman, B.R. (2005). The Effect of Shear on Dewatering of Flocculated Suspensions, PhD thesis, Department of Chemical and Biomolecular Engineering, The University of Melbourne, Melbourne, Australia.

[30] Slottee, J.S. and Johnson, J., Paste Thickener technology for mine backfill

[31] Slottee, J.S., Johnson, J. and Crozier, M. (2005). Paste Thickening Iron Ore Tailings, XXXV Iron Making and Raw Materials Seminar, VI Brazilian Symposium on Iron Ore, Brazil, pp. 1-8.

[32] Slottee, J.S. (2004). Update on the Application of Paste Thickeners for Tailings Disposal - Mine Paste Backfill, International Seminar on Paste and Thickened Tailings Paste and Thickened Tailings Paste, South Africa, pp.1-7.

[33] Nasser, M.S. and James, A.E. (2007). Numerical Simulation of the Continuous Thickening of Flocculated Kaolinite Suspensions, International Journal of Mineral Processing, 84, pp. 144–156.

[34] Usher, S.P., Spehar, R. and Scales, P.J. (2009). Theoretical analysis of aggregate densification: Impact on thickener performance, Chemical Engineering Journal, 151, pp. 202–208.

[35] Gladman, B.R., Rudman, M. and Scales, P.J. (2010). Experimental validation of a 1-D continuous thickening model using a pilot column, Chemical Engineering Science, 65, pp.3937–3946.

[36] Doucet J. and Paradis R. (2010). Thickening/ mud stacking technology- an environmental approach to residue management, 13th International seminar on paste and thickened tailings, Canada, pp. 1-20.

[37] Lester, D.R., Rudman, M. and Scales, P.J. (2010). Macroscopic dynamics of flocculated colloidal suspensions, Chemical Engineering Science, 65, pp. 6362–6378.

[38] Deventer, B.G., Usher, S.P., Kumar, A., Rudman, M. and Scales, P.J. (2011). Aggregate densification and batch settling, Chemical Engineering Journal, 171, pp. 141–151.

[39] Mcfarlane, A., Bremmell, K. and Addaimensah, J. (2005). Microstructure, rheology and dewatering behavior of smectite dispersions during orthokinetic flocculation, Minerals Engineering, 11, pp. 1173-1175.